

Exploration of orbital phase-dependent gamma-ray emission from the Black Widow Pulsar



E. M. H. Wu¹, J. Takata¹, K. S. Cheng¹, R. H. H. Huang², C. Y. Hui³, A. K. H. Kong², P. H. T. Tam², and J. H. K. Wu²

¹Department of Physics, University of Hong Kong, Pokfulam Road, Hong Kong

²Institute of Astronomy and Department of Physics, National Tsing Hua University, Hsinchu, Taiwan

³Department of Astronomy and Space Science, Chungnam National University, Daejeon, Republic of Korea

Abstract

Black widow pulsars are millisecond pulsars in a binary system with white dwarfs of mass less than ~ 0.1 solar mass. It is thought that the ultra-relativistic pulsar wind blows off the atmosphere of the companion, which eventually evaporates away. The acceleration process of the pulsar wind is not well established since there has been no direct observation of emission from the pulsar wind. By using the Fermi Large Area Telescope, we have found evidence on detection of γ -ray emission of the pulsar wind from the Black Widow Pulsar PSR B1957+20, which is modulated with the orbital phase of the binary at energies above ~ 2.7 GeV. It is suggested that the orbital phase-dependent γ -ray emission is produced in the intra-binary region via the inverse-Compton process.

Introduction

The Fermi Large Area Telescope (LAT) has measured pulsed γ -ray emission from millisecond pulsars (MSPs). The population is growing as more MSPs have been discovered by radio searches in Fermi unidentified sources. Recently, Guillemot et al. (2012) reported pulsed γ -ray emission from PSR B1957+20, the first “black widow” system, in which the MSP is destroying its low mass companion star. As at least 10 black widow systems have been discovered in the Fermi unidentified sources (Roberts 2011, Ray et al. 2012). In addition, Huang et al. (2012) found a modulation of the unresolved X-ray emission, discovered by Stappers et al. (2003), at the orbital period of ~ 9.2 hr, suggesting the origin of an intra-binary shock (Harding & Gaisser 1990; Arons & Tavani 1993; Cheng et al. 2006). The high-energy emission associated with an intra-binary shock between a pulsar and its companion star has been detected from the γ -ray binary PSR B1259-63, which consists of a canonical pulsar and a high-mass Be star (Johnston et al. 1992; Aharonian et al. 2009; Uchiyama et al. 2009). The γ -ray emission associated with the pulsar wind in the black widow system PSR B1957+20 has not been reported yet. We report evidence on orbital phase-dependence of GeV γ -ray emission from PSR B1957+20 detected by the Fermi LAT.

Spectral Analysis

Fermi-LAT data were taken between 2008 Aug 4 and 2011 Dec 5 (40 months) and reduced using the Fermi Science Tools v9r23p1. Photon energies were restricted to > 200 MeV and a region-of-interest of radius 5 degrees was used. An orbital cycle was divided into two parts: half containing the superior conjunction (“Phase 1”) and the other half containing the inferior conjunction (“Phase 2”). We performed unbinned analysis to fit the spectrum averaged over each orbit segment by a power-law with an exponential cut-off (PLE) model:

$$\frac{dN}{dE} = N_0 \left(\frac{E}{0.2 \text{ GeV}} \right)^{-\Gamma} \exp\left(-\frac{E}{E_c}\right).$$

The best-fit parameters are presented in Table 1. The difference in the cut-off energies suggests that the spectrum of Phase 2 extends to higher energies than that of Phase 1. This motivated the fitting for Phase 2 with a two-component model, which consists of a PLE with its power-law index and cut-off energy fixed at the best-fit values for Phase 1, and a Gaussian function:

$$\frac{dN}{dE} = A \exp\left[-\frac{(E - E_G)^2}{\sigma_G^2}\right].$$

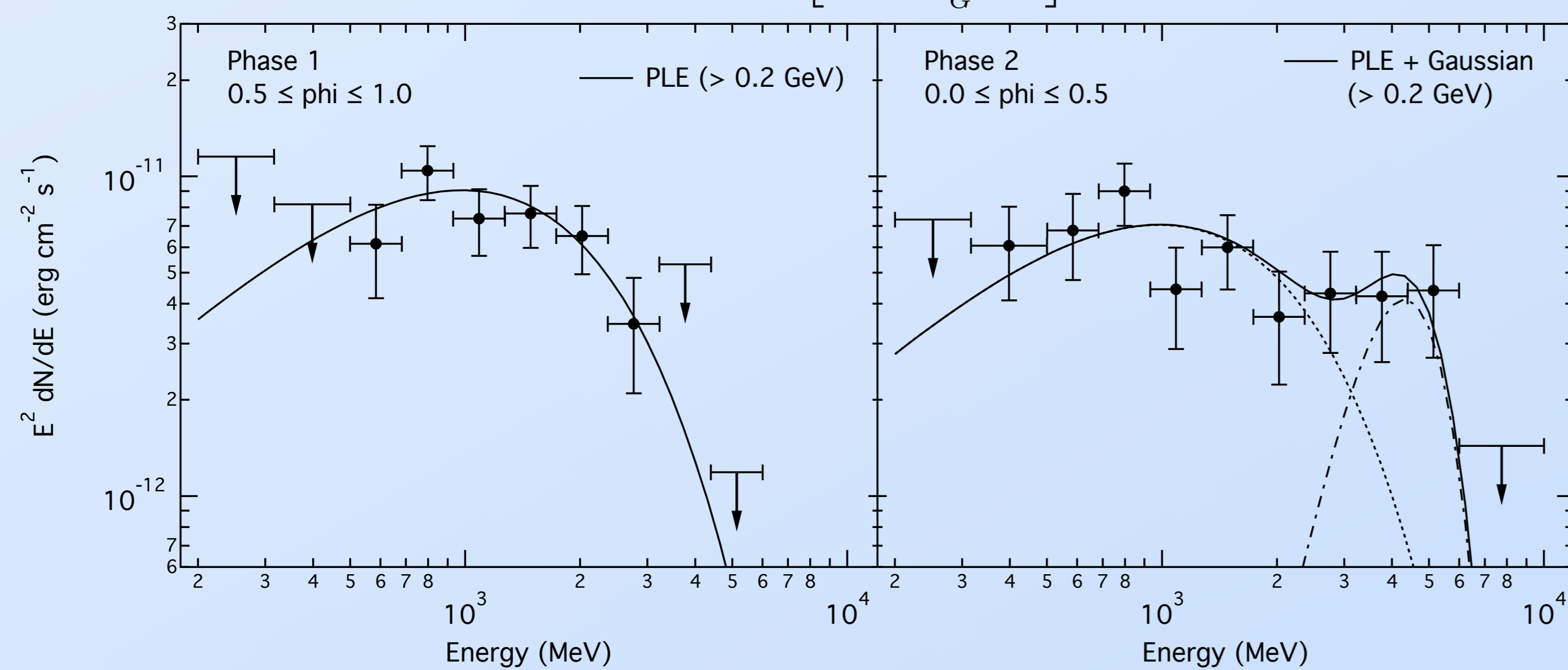


Figure 1. γ -ray SEDs of PSR B1957+20. **Left:** Spectrum averaged over Phase 1. The solid line represents the best-fit PLE model. **Right:** Spectrum averaged over Phase 2. The solid line represents the fitted two-component model; the PLE component is shown as the dashed line and the Gaussian component is shown as the dash-dotted line.

Orbital phase	Spectral index	Cut-off energy (GeV)	E_G (GeV)	σ_G (GeV)
Phase 1	0.83 ± 0.56	0.84 ± 0.30	---	---
Phase 2 (A)	1.58 ± 0.30	2.28 ± 0.88	---	---
Phase 2 (B)	0.83	0.84	3.76 ± 0.59	1.10 ± 0.39

Table 1. Summary of spectral fitting results of the two orbital phases.

Model (A): a single PLE model. **Model (B):** a PLE model + Gaussian function.

References

- Aharonian, F., et al. 2009, A&A, 507, 389
- Arons, J., & Tavani, M. 1993, ApJ, 403, 249
- Cheng, K. S., Taam, R. E., & Wang, W. 2006, ApJ, 641, 427
- Guillemot, L., Johnson, T. J., Venter, C., et al. 2012, ApJ, 744, 33
- Harding, A. K., & Gaisser, T. K. 1990, ApJ, 358, 561
- Huang, R. H. H., Kong, A. K. H., Takata, J., et al. 2012, arXiv:1209.5871
- Johnston, S., Manchester, R. N., Lyne, A. G., et al. 1992, ApJ, 387, L37
- Kataoka, J., Yatsu, Y., Kawai, N., et al. 2012, ApJ, 757, 176
- Kong, A. K. H., Huang, R. H. H., Cheng, K. S., et al. 2012, ApJ, 747, L3
- Ray, P. S., Abdo, A. A., Parent, D., et al. 2012, arXiv:1205.3089
- Roberts, M. S. E. 2011, API Conference Proceedings of Pulsar Conference 2010 “Radio Pulsars: a key to unlock the secrets of the Universe”, Sardinia, October 2010 (arXiv:1103.0819)
- Romani, R. W. 2012, ApJ, 754, L25
- Romani, R. W., & Shaw, M. S. 2011, ApJ, 743, L26
- Stappers, B. W., Gaensler, B. M., Kaspi, V. M., van der Klis, M., & Lewin, W. H. G. 2003, Sci, 299, 1372
- Uchiyama, Y., Tanaka, T., Takahashi, T., et al. 2009, ApJ, 698, 911

E. M. H. Wu et al. 2012, ApJ, accepted
Manuscript available at:
arXiv:1210.7209

Emission at High Energies

We constructed a pulse profile by phase-folding the photons with energies > 0.2 GeV within 1 degree from the position of PSR B1957+20. Data were excluded within the full widths at half-maximum of the two pulse peaks, which were fitted with Lorentzian functions. We compared the significance of emission below and above 2.7 GeV by computing the Test-Statistic (TS) maps (Figure 2).

The folded γ -ray lightcurve of PSR B1957+20 is presented in Figure 3. An optimized aperture radius of 0.965 deg gives an H-test TS of 19, corresponding to a significance of $\sim 3.3\sigma$. The post-trial significance is $\sim 2.3\sigma$.

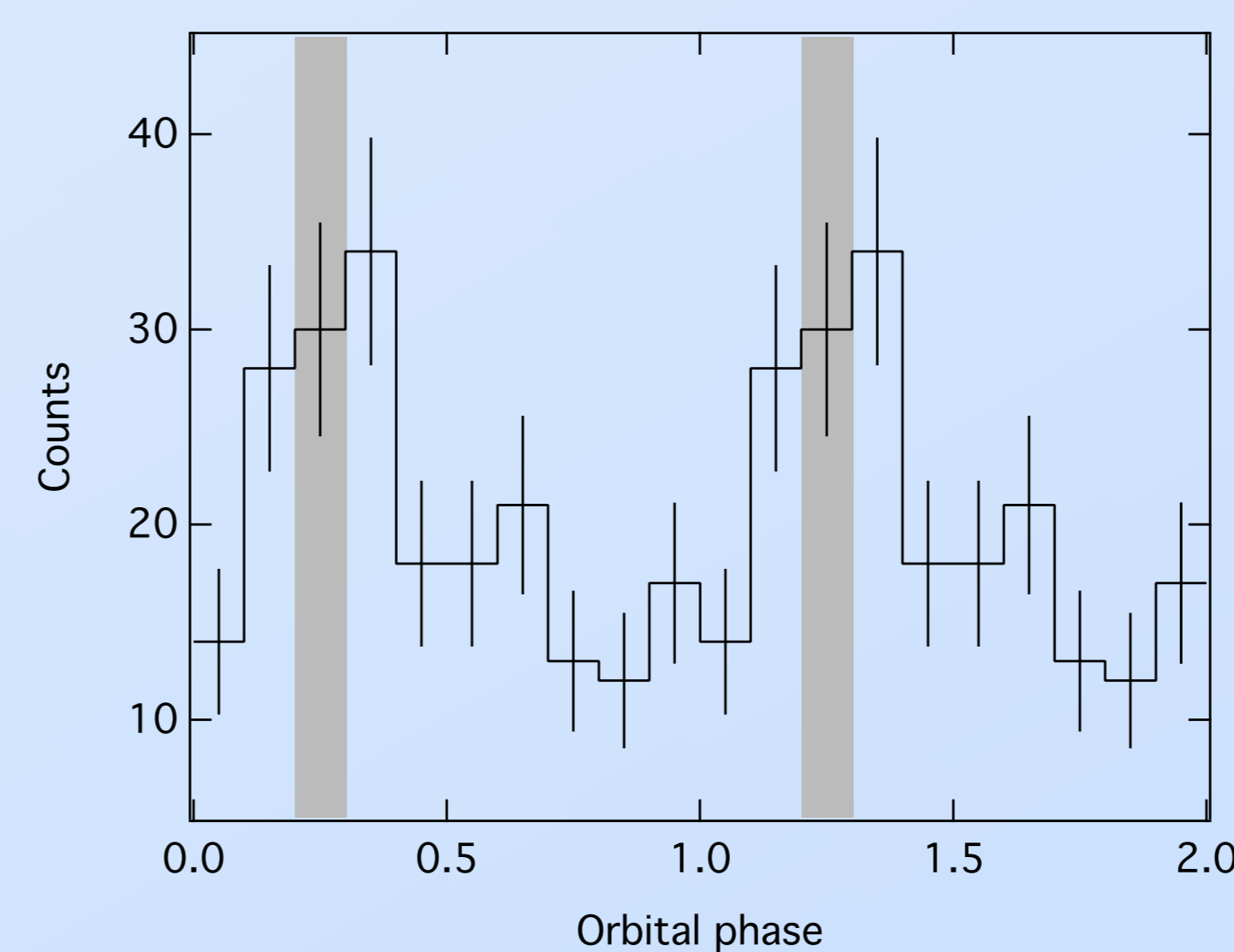


Figure 3. Folded lightcurve using the Fermi plug-in for TEMPO2, with an aperture size of 0.965 deg. The shaded regions correspond to the phase of radio eclipse, which is the center of Phase 2.

Discussion

A “cold” pulsar wind consisting of electron and positron pairs can convert its kinetic energy to internal energy in a shock by interacting with the inter-stellar medium. In pulsar wind nebulae, the shocked pulsar wind can produce X-rays via synchrotron radiation, which can be observed. The un-shocked cold pulsar wind, on the other hand, is dark in the X-ray band. However, in a binary system, the wind can emit very high-energy γ -rays by the inverse-Compton process between the cold pulsar wind and the background soft-photons from its companion. At the inferior conjunction passage, since the companion is located between the pulsar and the Earth, the inverse-Compton process occurs with head-on collision, whose emission dominates over the curvature radiation at energies > 3 GeV. In Phase 1, on the other hand, the inverse-Compton process occurs with tail-on collision, suppressing its emission at high energies.

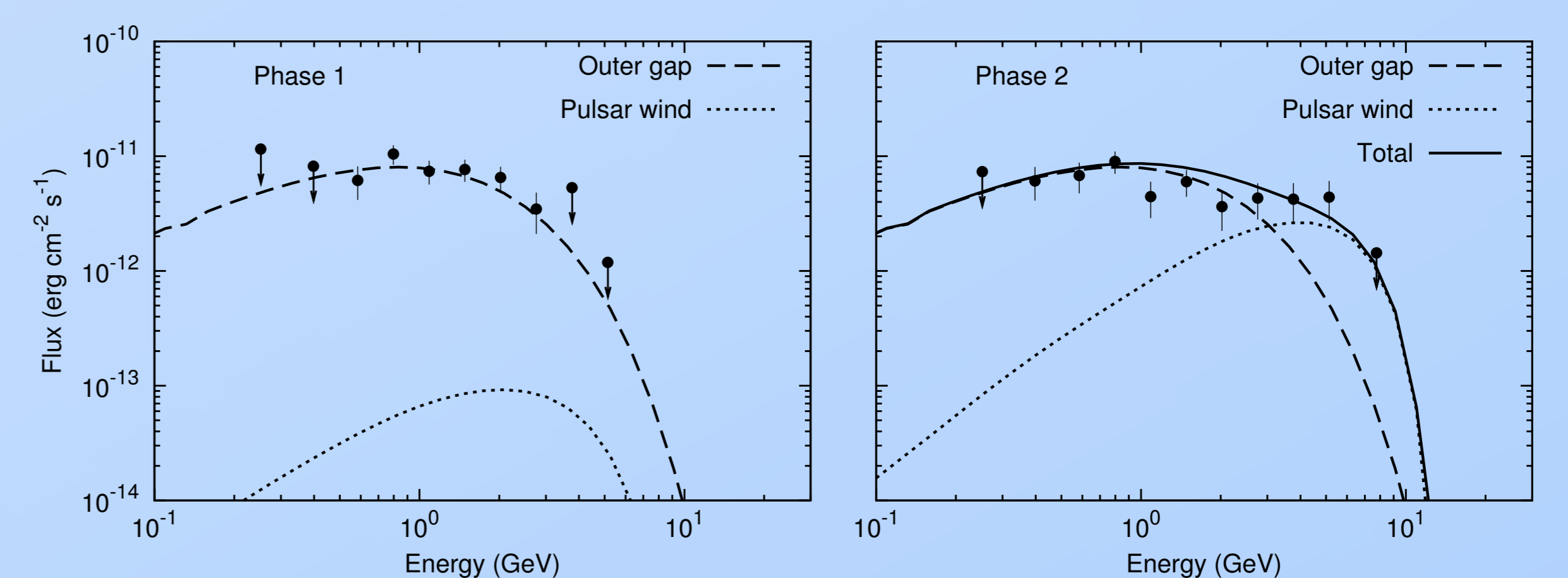


Figure 4. The dashed and the dotted lines are the spectra of the emission from the outer gap and the cold ultra-relativistic pulsar wind, respectively. The solid line represents the total contribution from the components.

Black widow pulsars discovered in Fermi unidentified sources are good targets for searching orbital phase-dependent γ -ray spectra, provided that accurate ephemerides are available. In addition, we note that orbital modulation of optical emission was found in the black widow candidates 2FGL J2339.6-0532 (Romani & Shaw 2011; Kong et al. 2012a) and 2FGL J1311.7-3429 (Kataoka et al. 2012; Romani 2012), and it is evident that the former candidate shows X-ray modulation as well. These systems are an excellent probe for γ -ray emission with both magnetospheric and pulsar wind components, by investigating the similarities and differences of their emission as a whole.

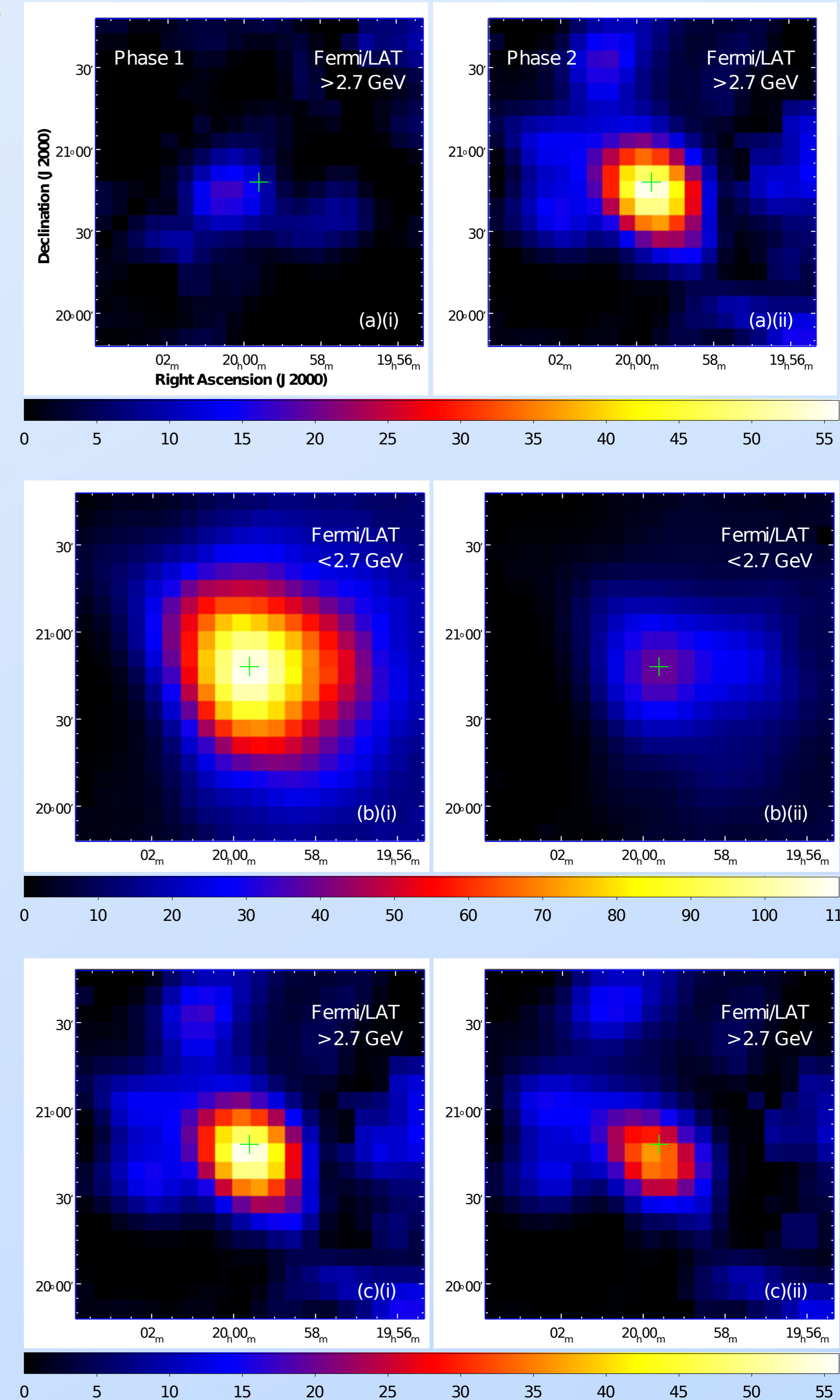


Figure 2. Test-Statistic maps of PSR B1957+20. **(a): (i)** At energies > 2.7 GeV for Phase 1. **(ii)** Same as (a)(i) but for Phase 2. **(b): (i)** At energies < 2.7 GeV for Phase 2. **(ii)** Same as (b)(i) but with FWHM of pulsation peaks removed. **(c):** Same as (b) but at energies > 2.7 GeV.